JVST A
Journal of Vacuum Science & Technology A

ARTICLE

avs.scitation.org/journal/jva

Ultraviolet photo-enhanced atomic layer deposition for improving dielectric properties of low temperature deposited Al_2O_3

Cite as: J. Vac. Sci. Technol. A 40, 040401 (2022); doi: 10.1116/6.0001865
Submitted: 17 March 2022 · Accepted: 22 April 2022 ·
Published Online: 13 May 2022

Konner E. K. Holden,[1,a)] Shane M. Witsell,[1] Paul C. Lemaire,[2] and John F. Conley, Jr.[1,b)]

AFFILIATIONS

[1]School of Electrical Engineering and Computer Science, Oregon State University, Corvallis, Oregon 97331
[2]Lam Research Corporation, Tualatin, Oregon 97062

[a)]**Present address:** Lam Research Corporation, Tualatin, Oregon 97062.
[b)]**Author to whom correspondence should be addressed:** jconley@eecs.oregonstate.edu

ABSTRACT

Thin films of Al_2O_3 are deposited using *in situ* ultraviolet (UV) light enhanced atomic layer deposition (ALD) with trimethylaluminum and H_2O and compared to those deposited using traditional thermal ALD at low temperatures of 45 and 80 °C. Coexposing the UV light with the H_2O pulse enhanced the growth-per-cycle and refractive index. Metal/insulator/metal devices using the *in situ* UV enhanced Al_2O_3 films demonstrated a reduction in leakage current at ±1 MV/cm by nearly an order of magnitude at a deposition temperature of 45 °C as compared to standard thermal ALD films as well as thermal ALD films that received a postdeposition (*in vacuo*) UV exposure. In addition, capacitance–voltage behavior of UV enhanced Al_2O_3 showed a dramatic reduction in capacitance–voltage hysteresis. Taken together, these electrical results suggest that *in situ* UV enhanced ALD of Al_2O_3 results in a reduced density of electrically active defects that likely arise from incorporated H and potentially other organic impurities left by incomplete surface reactions. This proof-of-concept approach could enable low temperature fabrication of metal/insulator/metal and other devices in temperature-sensitive applications such as flexible electronics.

I. INTRODUCTION

Atomic layer deposition (ALD) is based on alternating purge-separated injections of gaseous precursors, selected such that they result in self-limiting thermally driven surface reactions with volatile and inert by-products. The cyclic nature of ALD combined with self-termination allows deposition of high quality, highly uniform, and conformal films over extreme topography and large areas, and atomic scale thickness control with typical growth-per-cycle (GPC) of less than a monolayer of film. For thermal ALD processes, deposition temperatures typically fall within the range of 100–400 °C.[1] While this fairly low temperature range is considered an advantage and meets present-day complementary metal oxide semiconductor (CMOS) requirements, low deposition temperatures can result in poor film stoichiometry due to the incorporation of excess OH groups or other residual impurities from unreacted precursor ligands as a consequence of reduced thermal energy. These incorporated impurities, in turn, can lead to suboptimal physical, optical, and electrical properties.[1,2] For deposition on flexible substrates (e.g., polyethylene terephthalate, used for thin film solar cells), even lower temperatures can be required due to the low melting, glass transition, or decomposition temperatures of these materials.

A number of approaches may be used to reduce impurities, increase density, improve properties, and achieve desired stoichiometry of ALD films. The most common approach is postdeposition annealing (PDA) at elevated temperatures. However, the PDA temperatures that are typically required can exceed the maximum temperature limitations of the substrate or of previously formed electronics. One approach to improving ALD film quality while simultaneously maintaining a low thermal budget is the use of additional energy sources. Some widely used examples include plasma enhanced ALD (PEALD)[3] and the use of other oxidants such as ozone, both leveraging species with higher reactivity to

drive the lower-temperature surface reactions. However, PEALD and ozone-based processes are limited by drawbacks such as damage to polymer substrates or bottom metal electrodes due to ion bombardment[4] or interfacial layer formation due to surface oxidation.[5,6] Another approach involving *in situ* thermal annealing, in which rapid thermal anneal (RTA) or flash lamp exposures are performed every or every few ALD cycles, has been demonstrated to produce improved properties at a lower thermal budget. Originally termed modulated temperature annealing MTA-ALD, but now often referred to as dep-anneal-dep-anneal (DADA), *in situ* thermal annealing may be impractical for high volume manufacturing due to the long post-RTA wait times required to cool back down to the ALD process temperature.[7–10] A closely related technique, *in situ* flash lamp enhanced ALD, uses shorter heating pulses to dissociate reactants but can be more akin to pulsed CVD, losing some of the inherent benefits of ALD.[11] Given that these methods are not specifically driving surface reactions during ALD, they add significant process time overhead, which in ALD is already significant.

Other methods to drive reactions, reduce impurity/ligand incorporation, and improve ALD film quality *in situ* during deposition while maintaining low thermal budget include nonthermal methods such as plasma treatments [known as atomic layer annealing (ALA)], laser annealing, electron beam exposure, and ultraviolet (UV) light exposure.[12–23] UV light, in particular, has been demonstrated as an alternative energy source in UV photo-enhanced ALD (UV-ALD). UV photons at wavelengths less than 200 nm are energetic enough to break C–H, C–C, and O–H bonds and can rapidly remove adsorbed species such as H, OH, and H_2O.[21–24] UV can be used to enable photolytic "single-source" ALD processes consisting of alternating precursor pulse/purge/UV exposure/purge for materials such as TiO_2, Ta_2O_5, ZrO_2, HfO_2, Nb_2O_5, ZnO, and Al_2O_3,[16,25–27] a metalorganic precursor with UV excitation of O_2 as a reactant,[28,29] or to enable[27] or enhance surface reactions.[12,30–32] UV-ALD has been demonstrated to enable deposition of high-quality Al_2O_3 using TMA and O_2 through the photoexcitation of O_2 molecules into more reactive O species,[28] and to assist in the H_2O/surface methyl group reaction in the TMA/H_2O process.[17] The O_2 process was reported at a deposition temperature of 60 °C and the H_2O process 40 °C, and both exhibited GPC, refractive index (RI), and H impurity concentrations nearing levels of the thermal TMA/H_2O and TMA/O_3 processes deposited at much higher temperatures (>200 °C).[2,33]

A potential consideration is the directionality of the UV light. For UV-*enhanced* ALD processes, deposition would still occur in areas which are shadowed. Because they are not exposed to UV photons, the film in such areas would suffer from poorer material quality, but this could possibly be exploited, e.g., for etch selectivity. On the other hand, directionality can be beneficial for a UV *enabled* ALD process where UV photons are necessary for deposition. Such processes have been demonstrated to enable area selective deposition (the direct deposition of a pattered film without a photoresist process).[16,26,28]

It is widely understood that exposure of dielectrics to UV radiation can have detrimental effects on electrical properties such as charge trapping.[34] It is, therefore, important to make direct comparisons of electrical properties of films deposited using UV-ALD versus standard thermal ALD processes. Despite several reports on the impact of UV exposure on growth and material properties, there have been very few reports of the effect on electrical properties. While Lee *et al.* report leakage current for a UV *enabled* ALD ZrO_2 MOS capacitor, a comparison to films deposited via thermal ALD could not be made as films could not be deposited via standard thermal ALD using the same chemistry.[27] No *et al.* investigated the addition of UV exposure during the purge steps of an ALD TMA/H_2O process performed at a high deposition temperature of 370 °C. They reported reduced electrical leakage current and increased the extracted barrier height for Fowler Nordheim tunneling (FNT) in the UV ALD films as compared to the thermal ALD films.[32] However, as 370 °C is above the decomposition threshold temperature of TMA, thermal ALD films of Al_2O_3 deposited at this temperature contain excess C due to the decomposition of adsorbed precursors and improvements in electrical properties were mainly attributed to the UV photoexcitation induced elimination or photodissociation of excess C groups on the surface.

In this work, UV-enhancement of low temperature (45 and 80 °C) ALD Al_2O_3 processes is investigated and compared with standard thermal ALD at the same temperatures. GPC and RI values are compared between UV- and thermal ALD films. Using MIM devices for electrical characterization, current–voltage (*I-V*) and capacitance–voltage (*C-V*) measurements were carried out to examine the impact of UV enhancement on current leakage, dielectric constant, and capacitance–voltage nonlinearities.

II. EXPERIMENT

ALD of Al_2O_3 was performed in a modified Picosun R-200 hot-wall, continuous N_2 flow reactor operated at ~1 Torr, shown schematically in Fig. 1, using alternating N_2 purge-separated cycles of TMA and H_2O. TMA and H_2O were delivered via stainless steel vapor draw sources held at lab temperature (23–25 °C).

A 1000 W Xe(Hg) arc lamp (Newport Corp.) provided broadband (190–3000 nm) emission in a nearly collimated beam of approximately 2 in. diameter. Light from the arc lamp source was passed into the vacuum chamber through a UV-grade fused silica (UVFS) viewport to allow wavelengths as short as 180 nm to pass into the chamber. The lamp-to-wafer distance was approximately 1 m. To prevent deposition on the viewport, nearby N_2 flow was supplied by a directly attached side-ported flange (also in Fig. 1). For indicated depositions, the beam was also passed through a 250–500 nm UV band pass filter from Thorlabs which rejected wavelengths below 250 nm and between 500–650 nm. Optical power density was measured under atmospheric, open-chamber conditions to be 2 W/cm^2 at the center of the substrate holder, where the beam was most intense. Note that light is reflected throughout the deposition chamber. Light exposures were performed automatically using a servo-driven shutter controlled by a microcontroller that listened to the ALD reactor's logic signals during precursor injection.

Exposure to the light beam was found to increase the temperature of the wafer during exposures after which the sample cools until the next exposure. See Fig. S1 in the supplementary material[48] detailing this behavior. To avoid unintended photo-thermal effects and provide a "temperature matched" comparison between

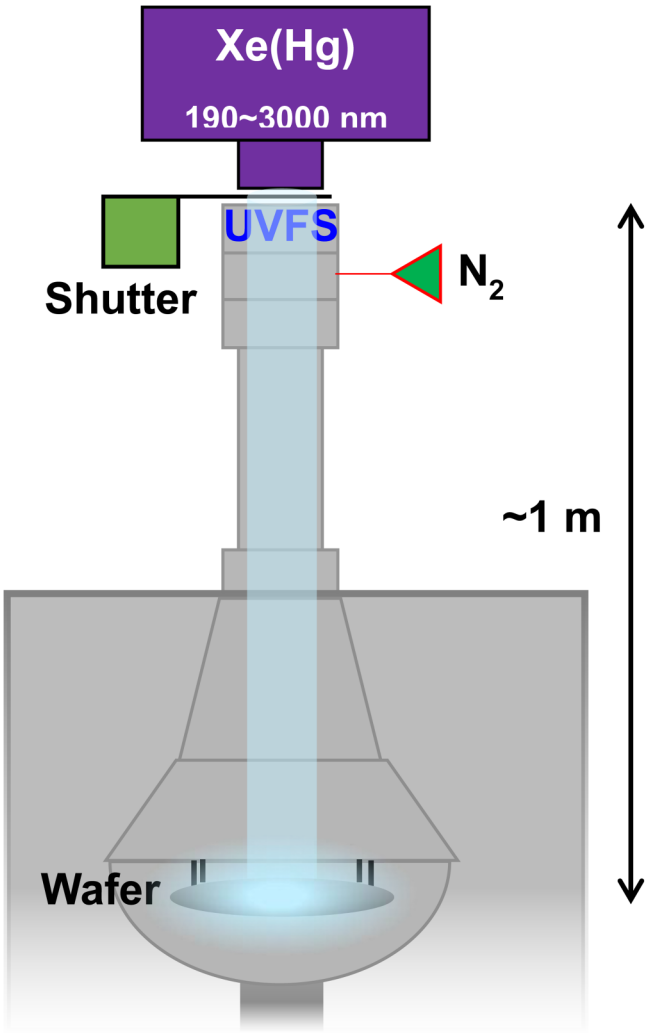

FIG. 1. Schematic of the ALD reactor used in this work, reconfigured to support a 1000 W Xe(Hg) arc lamp directly above the wafer.

UV-ALD photo-chemical effects and thermal ALD, this temperature increase was accounted for by setting the chamber temperature for the thermal ALD runs to be equal to the maximum temperature reached during UV-ALD deposition. Note that because the maximum UV-ALD wafer temperature was used for this comparison, the thermal ALD wafers were at a higher overall average temperature during deposition.

Ellipsometry was performed *ex situ* using a single-angle, multiwavelength FS-1 ellipsometer from FilmSense. Measurements were made on 1 in. × 1 in. Si witness coupons with ~1.6 nm native SiO_2 placed alongside device samples in each run. Al_2O_3 thickness and RI were extracted from a Cauchy dispersion model and a separate model was applied to account for the native SiO_2 layer.

$Si/SiO_2/Ti/TiN$ substrates (<0.4 nm RMS) provided by ON Semiconductor were used as bottom electrode substrates for device

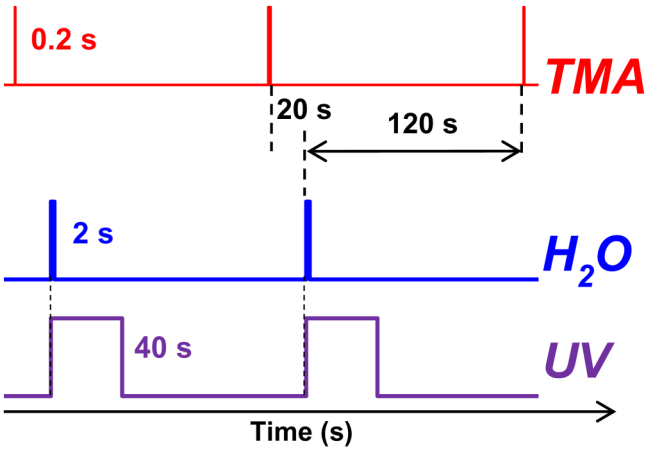

FIG. 2. Pulsing scheme for UV-ALD and thermal ALD processing used in this work. N_2 (not shown) is supplied continuously throughout pulse and purge steps.

fabrication. Following ALD or UV-ALD of Al_2O_3 onto the bottom TiN electrodes, top electrodes of Pt were electron-beam evaporated at a base pressure of 10^{-7} Torr through circular shadow masks of 250 μm diameter to complete MIM device fabrication.

Current versus voltage (I–V) and 100 kHz capacitance versus voltage (C–V) measurements were taken using a probe station in a dark box with an Agilent 4156C semiconductor parameter analyzer and 4284A LCR meter, respectively. Optical microscope images of the circular top electrodes were used to determine electrode area for calculations of current and capacitance density (J and C_d, respectively), while the ellipsometric thickness of Al_2O_3 was used for calculating electric field, ξ.

III. RESULTS AND DISCUSSION

Standard thermal and UV enhanced ALD were performed at matched (described in Sec. II) wafer temperatures, T_{wafer}, of 45 and 80 °C to determine the impact of UV enhancement on the Al_2O_3 film and MIM device properties. Identical ALD pulsing parameters of 0.2 s TMA pulse/20 s N_2 purge/2 s H_2O pulse/120 s N_2 purge were used, with the exception of the added 40 s UV pulse, which begins at the start of the H_2O pulse and ends during the 120 s N_2 purge (shown schematically in Fig. 2).

Table I lists the GPC and RI values obtained in this work using single film thickness measurements (assuming no nucleation delay) for Al_2O_3 deposited at *matched* (see description above) deposition temperatures of 45 and 80 °C via UV-ALD without the optical filter and thermal ALD, along with previous literature reports. For depositions at 80 °C, we observe in the UV enhanced films an increase in GPC from 0.95 to 1.05 Å/cycle and a slight increase in RI from 1.60 to 1.62. The presence or absence of the optical filter had no significant effect.

Comparing to the work by Yoon *et al.* for a nearly identical TMA and H_2O process (UV exposure during and following only the H_2O pulse), the GPC and RI differences between UV enhanced and thermal ALD are less pronounced,[17] as shown in Table I. It is

TABLE I. Reports of GPC and RI for low temperature thermal and UV enhanced ALD Al_2O_3.

	GPC (Å/cycle)		RI		
T_{wafer} (°C)	Thermal	UV	Thermal	UV	Reference
40	0.8	1.3	1.58	1.66	Yoon *et al.* (Ref. 17)
45	0.95	1.00	1.60	1.60	This work
77	0.98	—	—	—	Ott *et al.* (Ref. 36)
80	0.98	1.05	1.60	1.62	This work
	0.9	—	1.59	—	Yoon *et al.* (Ref. 17)
	1.3	—	1.55	—	Groner *et al.* (Ref. 2)

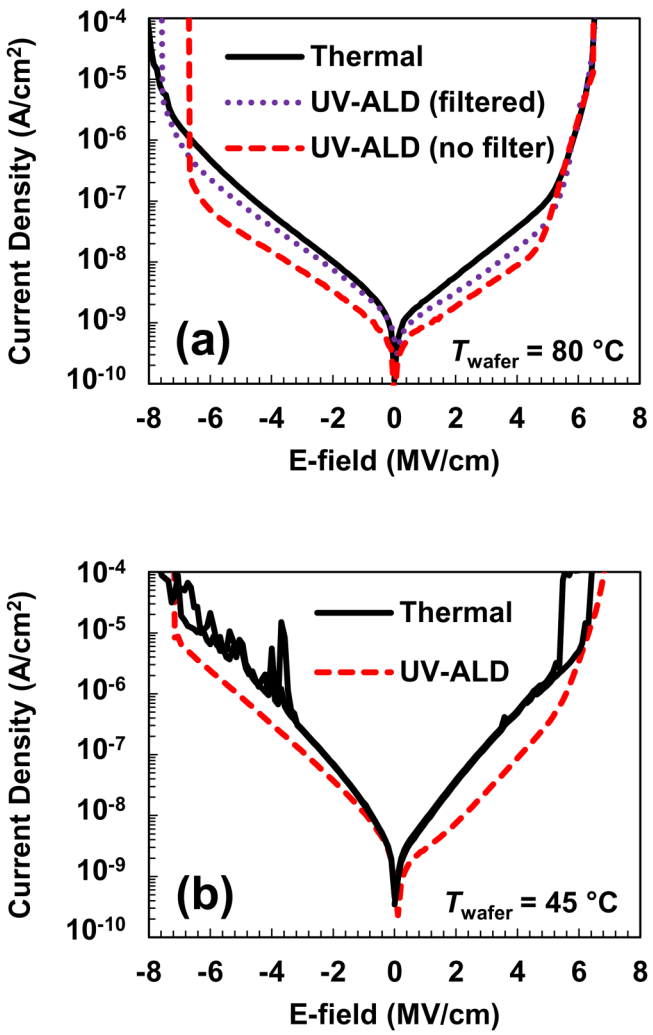

FIG. 3. (a) Log J-ξ plots comparing TiN/Al_2O_3/Pt devices with Al_2O_3 films deposited at T_{wafer} = 80 °C using a thermal and UV-ALD process with and without an optical filter, as indicated. (b) Log J-ξ plots of an identical device structure deposited at T_{wafer} = 45 °C comparing a thermal and UV-ALD process without an optical filter.

possible the UV exposure in our work is not completely saturated, due to a lower optical power density. Despite the longer UV exposure time (40 s here versus 2 to 6 s in Yoon *et al.*), the 10× shorter lamp-to-wafer distance of 10 cm in the work by Yoon *et al.* provides a higher surface optical power density of ~4 W/cm^2 as compared to ~2 W/cm^2 in this work. It is noted that reactor-specific or measurement-specific conditions can also influence ALD GPC and material properties.[35] As indicated in Table I, previous reports of low-temperature ALD Al_2O_3 show significantly different GPC and RI using nominally the same process. For deposition at 80 °C, the GPC of 0.98 Å/cycle we find for standard thermal ALD is the same as reported by Ott *et al.*, quite a bit less than the 1.3 Å/cycle reported by Groner *et al.* (incidentally, from the same lab as Ott *et al.* but using a different reactor), and higher than the 0.9 Å/cycle reported by Yoon *et al.* The lower RI of 1.55 and much higher GPC of 1.3 Å/cycle reported by Groner *et al.* suggests that precursor cross talk due to H_2O condensation may be playing a role in this temperature regime. Indeed, Groner *et al.* reported reduced RI, film density, and dramatically increased hydrogen content as ALD temperature was lowered.[2] The consistent RI = 1.6 reported here and by Yoon *et al.* suggest films of comparable quality. Despite the variation in GPC reported for thermal ALD Al_2O_3, UV exposure has a clear influence on GPC and possibly a marginal influence on RI.

Next, as a more sensitive probe of impurity and defect reduction than the bulk GPC and RI measurements, the electrical properties of UV-ALD and thermal ALD films were compared using TiN/Al_2O_3/Pt MIM devices. Shown in Fig. 3 are representative J–ξ plots for MIM devices with 10 nm thick Al_2O_3 layers deposited at the matched temperatures of (a) 80 °C and (b) 45 °C. An overall reduction in leakage was observed at both temperatures for the UV-ALD films, consistent with improved film quality and a reduction in defect-based conduction. As seen in Fig. 3(a), the reduction

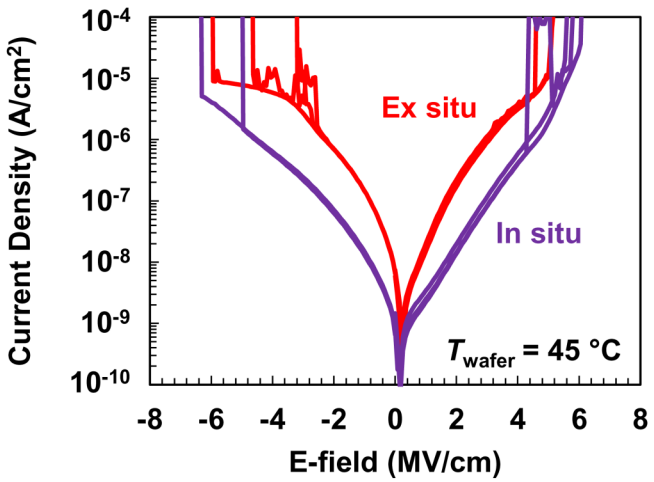

FIG. 4. Current density vs. electric field measurements for TiN/Al_2O_3/Pt MIM devices with Al_2O_3 layers deposited using either *in situ* or *ex situ* (as indicated) UV exposures during or after ALD, respectively.

in leakage was greater *without* the use of the optical filter, despite the less than one standard deviation difference in GPC and RI with or without the filter (1.03 Å/cycle versus 1.05 ± 0.02 Å/cycle and 1.616 versus 1.62 ± 0.005, respectively). Experiments with a surface mounted thermocouple (T/C) wafer, summarized in Fig. S1,[48] show that the wafer is heated to nearly the same temperature regardless of whether the filter is used. As UV exposure without the filter produces much lower leakage despite roughly the same wafer temperature as UV exposure with the filter, it appears that the wavelengths below 250 nm (attenuated by the optical filter) are responsible for the reduced leakage. Therefore, use of the optical filter, intended to prevent photothermal effects, is not desirable.

Note that the dielectric breakdown (the near vertical increase in leakage) occurring at approximately −6.6 MV/cm in the unfiltered UV-ALD film in Fig. 3(a) does not indicate reduced overall breakdown strength for these films. Dielectric breakdown is a statistical process and thus the breakdowns occurring in the representative curves shown for each device do not represent the mean dielectric breakdown strength.

A comparison to *ex situ* (postdeposition, *in vacuuo*) UV exposure was performed to verify the effectiveness versus the *in situ* UV exposures (during UV-ALD). Shown in Fig. 4 are current density versus electric field curves for TiN/Al_2O_3/Pt MIM devices in which Al_2O_3 ALD was performed at $T_{wafer} = 45$ °C with either *ex situ* (post deposition) or *in situ* (during ALD) UV exposures. For the *ex situ* experiment, the exact same UV exposure sequence as in Fig. 2 (but *without* the precursor dosing) was executed *after* standard thermal ALD to match the UV and thermal budget of the *in situ* UV exposures. The reduced current density in the *in situ* UV-ALD versus the *ex situ* UV exposed device demonstrates that UV exposure during ALD produces enhancements that cannot be achieved through postdeposition exposure. These data support a surface-driven process being responsible for the lower dielectric leakage current in the UV-ALD processed films.[17]

Representative C_d–V curves for the MIM devices are shown in Fig. 4. The relative dielectric constant, κ, was found to be roughly 7.3 and 7.1 for the films deposited at (a) 80 °C and (b) 45 °C, respectively, lower than 7.6–7.9 typically observed for thermal ALD

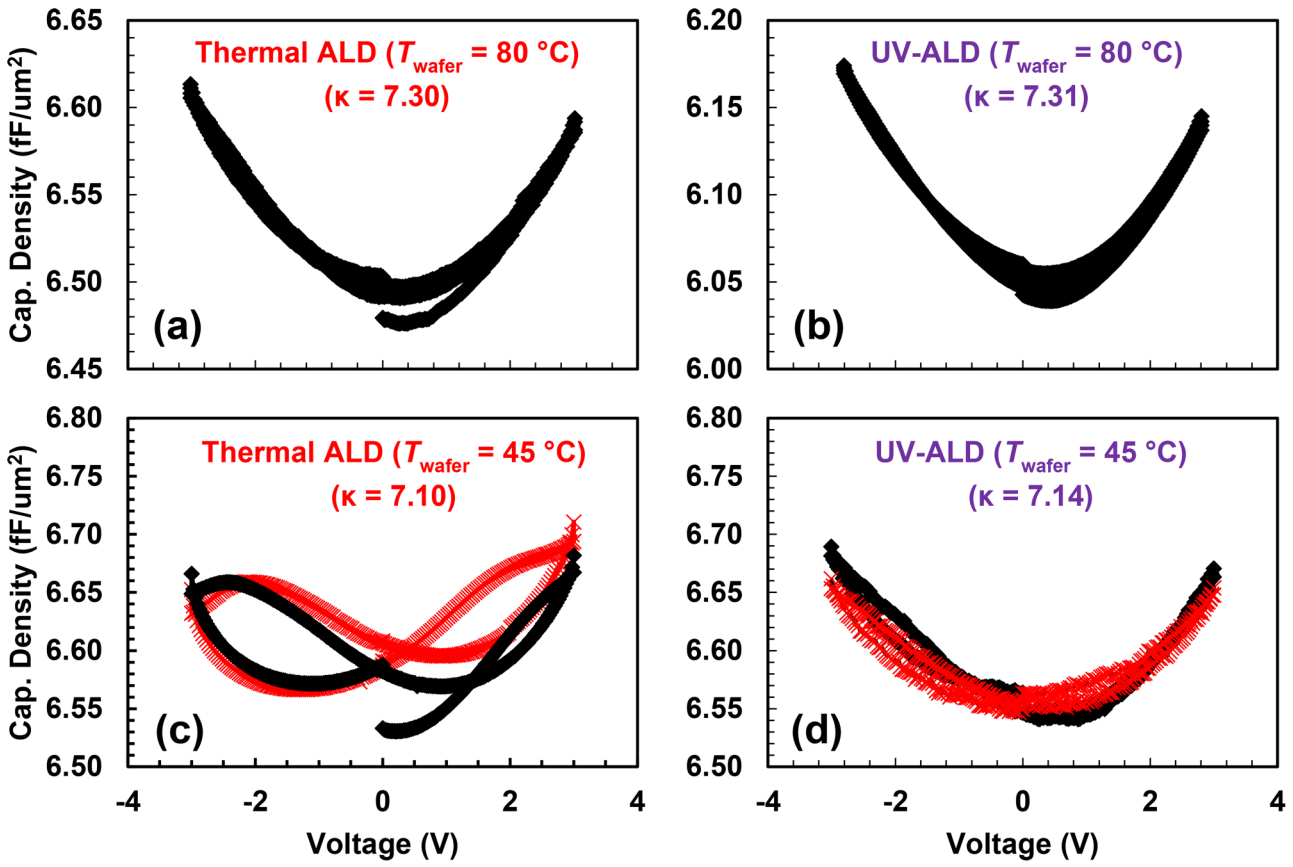

FIG. 5. C_d-V curves for (a) and (c) thermal and (b) and (d) UV-ALD at the indicated matched wafer temperatures. For the depositions at 45 °C in (c) and (d), the black diamonds and red "X" curves represent the first and second voltage sweeps, respectively.

Al_2O_3 deposited at 250–300 °C, and consistent with the general trend of reduction in κ as growth temperature is reduced.[37–39] No significant difference in κ was observed between the baseline thermal ALD films and the UV-ALD films at either temperature.

Despite the lack of change in dielectric constant, the impact of *in situ* UV exposure on the dielectric properties can be clearly seen in the 45 °C devices. The baseline thermal ALD process [Fig. 5(c)] shows an atypical "S"-shape *C-V* curve, the UV-ALD devices [Fig. 5(d)] shows the more typical parabolic *C-V* shape.[40] For MIM devices, the minimum capacitance value C_{min} has been correlated with the defect centroid position.[41,42] The voltage sweep direction-dependent hysteresis, shift in C_{min}, seen for the thermally processed device [Fig. 5(c)] strongly suggests that charged defects are present either as mobile ionic species or near-interfacial (switching) traps.[43,44]

Previous work has shown that low temperature thermal ALD Al_2O_3 typically has increased levels of hydroxyl and carbon content.[2,17] Yoon *et al.* used XPS to compare thermal and UV ALD films and found that thermal ALD films contained unreacted –OH groups while UV enhanced films contained mainly O–Al–O bonding and had an improved O/Al ratio (1.66 for UV versus 1.56 for thermal), reduced carbon content (0.07% versus 0.36%), and increased density (3.01 versus 2.59 g/cm^3). They concluded that the *in situ* UV exposure assisted reactions between H_2O and –O–Al $(CH_3)_2$ surface groups to form Al_2O_3 by removing $–CH_3$ groups via photo-dissociation.[45] They also found that by promoting reconstruction of surface groups through the release of H_2O and weakly bound reaction residues from the metal oxide surface, UV exposure dramatically reduced the time required for purging following the H_2O pulse.[17,24] The reduction of carbon content is consistent with that reported by No *et al* for Al_2O_3 deposited at high temperatures.[32]

Taken together, the reduction in defect-related charge transport at fields below the Fowler–Nordheim tunneling regime (for thermal and *ex situ* UV-treated films) and reduced CV hysteresis (Figs. 3–5, respectively) suggests that the *in situ* UV treatment reduced intrinsic and impurity defects, likely associated with oxygen vacancies and H and C impurities. The lack of change in κ indicates that the source of dielectric polarization at the 100 kHz measurement frequency is most likely not dominated by polarizable species relating to H impurities, as has been suggested elsewhere.[46,47]

IV. SUMMARY AND CONCLUSIONS

It has been known that the thermal ALD Al_2O_3 process using TMA and H_2O suffers from high H and C impurity incorporation and low density at lower deposition temperatures. Previous work has shown that by providing additional energy to the ligand exchange reaction between H_2O and surface methyl groups, *in situ* UV and photo-enhanced ALD processes can reduce H and C impurities, thereby improving stoichiometry and increasing film density. In this work, UV enhanced ALD of Al_2O_3 was compared to standard thermal ALD at low deposition temperatures of 45 °C and 80 °C. In confirmation of previous reports, we found an increase in ALD GPC and slight increase in refractive index of the photo-enhanced process over the thermal process.

Although there have been a number of reports of UV enhanced ALD of various materials, there have been fewer reports on the impact of UV exposure on electrical properties, and no direct comparisons of the impact of *in situ* UV on the TMA/H_2O process at low deposition temperatures. To directly measure the impact of UV enhancement on electrical properties, we fabricated TiN/Al_2O_3/Pt MIM devices. UV-ALD films were found to exhibit reduced leakage current, and films deposited at 45 °C show reduced C–V hysteresis. Both reduced leakage and hysteresis are consistent with a reduction in intrinsic and/or impurity related defects (C and H). Devices that were exposed postdeposition (*in vacuo*) did not show a reduction in leakage, consistent with a surface-driven photo-enhanced process.

Because the thermal ALD wafers were at a higher overall average temperature during deposition (the UV-ALD wafer reached the same temperature only at the end of each UV pulse and then cooled until the next pulse), the comparison presented provides a conservative estimate of the effects of UV exposure. Experiments with an optical filter indicated that wavelengths below 250 nm are required. The smaller effect on growth-per-cycle and refractive index compared to other reports of UV-enhanced ALD Al_2O_3 suggests that improvements in lamp and optics design, i.e., higher optical power density at shorter wavelengths and closer lamp-to-wafer distance (not feasible with our purpose-built plasma ALD reactor) would likely result in further improvement of electrical performance for these devices at lower temperatures. Nevertheless, this work provides a clear demonstration that *in situ* UV exposure can enhance the electrical properties of low temperature ALD Al_2O_3. These results confirm that UV can serve as an additional energy source to drive ALD reactions, remove loosely bonded residue from the growth surface, and help to achieve a more ideal ALD process. UV enhanced ALD may thus help enable temperature sensitive applications such as flexible electronics and back-end-of line 3D integration of transistors.

ACKNOWLEDGMENTS

The authors thank Zachary Steinberg of Oregon State University for early shutter controller development work, Jessica Peterson and Ben Kupp for assistance with electrical measurements, and Chris Tasker of Oregon State University for equipment support. The authors thank ON Semiconductor for supplying Si/SiO_2/Ti/TiN substrates. This work was supported in part by the Unlock Ideas program of Lam Research Corp. and conducted at the Materials Synthesis and Characterization (MaSC) Center, a National Nanotechnology Coordinated Infrastructure (NNCI) Northwest Nanotechnology Infrastructure (NWNI) user facility at the Oregon State University which is supported in part by the National Science Foundation (NSF) (Grant No. ECC-2025489) and Oregon State University.

AUTHOR DECLARATIONS

Conflict of Interest

The authors have no conflicts to disclose.

DATA AVAILABILITY

The data that support the findings of this study are available from the corresponding author upon reasonable request.

REFERENCES

[1]V. Miikkulainen, M. Leskelä, M. Ritala, and R. L. Puurunen, J. Appl. Phys. **113**, 021301 (2013).
[2]M. D. Groner, F. H. Fabreguette, J. W. Elam, and S. M. George, Chem. Mater. **16**, 639 (2004).
[3]V. Vandalon and W. M. M. Kessels, Appl. Phys. Lett. **108**, 011607 (2016).
[4]G. S. Oehrlein, R. J. Phaneuf, and D. B. Graves, J. Vac. Sci. Technol. B **29**, 010801 (2011).
[5]R. W. Johnson, A. Hultqvist, and S. F. Bent, Mater. Today **17**, 236 (2014).
[6]K. E. K. Holden and J. F. Conley, Jr., J. Vac. Sci. Technol. A **37**, 020903 (2019).
[7]J. F. Conley, Jr., Y. Ono, and D. J. Tweet, Appl. Phys. Lett. **84**, 1913 (2004).
[8]J. F. Conley, Jr., D. J. Tweet, Y. Ono, and G. Stecker, MRS Proc. **811**, 158 (2004).
[9]R. D. Clark, S. Consiglio, G. Nakamura, Y. Trickett, and G. J. Leusink, ECS Trans. **41**, 79 (2011).
[10]M. C. Langston, N. P. Dasgupta, H. J. Jung, M. Logar, Y. Huang, R. Sinclair, and F. B. Prinz, J. Phys. Chem. C **116**, 24177 (2012).
[11]T. Henke, M. Knaut, C. Hossbach, M. Geidel, L. Rebohle, M. Albert, W. Skorupa, and J. W. Bartha, ECS J. Solid State Sci. Technol. **4**, P277 (2015).
[12]J. K. Sprenger, H. Sun, A. S. Cavanagh, and S. M. George, J. Vac. Sci. Technol. A **36**, 01A118 (2018).
[13]J. Nishizawa, H. Abe, T. Kurabayashi, and N. Sakurai, J. Vac. Sci. Technol. A **4**, 706 (1986).
[14]J. Olander, L. M. Ottosson, P. Heszler, J.-O. Carlsson, and K. M. E. Larsson, Chem. Vap. Dep. **11**, 330 (2005).
[15]P. R. Chalker, Surf. Coat. Technol. **291**, 258 (2016).
[16]V. Miikkulainen, K. Väyrynen, V. Kilpi, Z. Han, M. Vehkamäki, K. Mizohata, J. Räisänen, and M. Ritala, ECS Trans. **80**, 49 (2017).
[17]K. H. Yoon, H. Kim, Y.-E. K. Lee, N. K. Shrestha, and M. M. Sung, RSC Adv. **7**, 5601 (2017).
[18]H.-Y. Shih, W.-H. Lee, W.-C. Kao, Y.-C. Chuang, R.-M. Lin, H.-C. Lin, M. Shiojiri, and M.-J. Chen, Sci. Rep. **7**, 39717 (2017).
[19]E. Österlund, H. Seppänen, K. Bespalova, V. Miikkulainen, and M. Paulasto-Kröckel, J. Vac. Sci. Technol. A **39**, 032403 (2021).
[20]S. T. Ueda, A. McLeod, D. Alvarez, D. Moser, R. Kanjolia, M. Moinpour, J. Woodruff, and A. C. Kummel, Appl. Surf. Sci. **554**, 149656 (2021).
[21]M. A. Henderson, Surf. Sci. Rep. **46**, 1 (2002).
[22]J. R. Vig, J. Vac. Sci. Technol. A **3**, 1027 (1985).
[23]R. E. Van de Leest, Appl. Surf. Sci. **86**, 278 (1995).
[24]J. F. Conley, Jr., IEEE Trans. Dev. Mater. Rel. **10**, 460 (2010).
[25]V. Miikkulainen, K. Väyrynen, K. Mizohata, J. Räisänen, M. Vehkamäki, and M. Ritala, J. Vac. Sci. Technol. A **37**, 060911 (2019).
[26]V. Miikkulainen, M. Vehkamäki, K. Mizohata, T. Hatanpää, and M. Ritala, Adv. Mater. Interfaces **8**, 2100014 (2021).
[27]B. H. Lee, S. Cho, J. K. Hwang, S. H. Kim, and M. M. Sung, Thin Solid Films **518**, 6432 (2010).
[28]P. R. Chalker, P. A. Marshall, K. Dawson, I. F. Brunell, C. J. Sutcliffe, and R. J. Potter, AIP Adv. **5**, 017115 (2015).
[29]Y.-H. Lee, J.-C. Kwak, B.-S. Gang, H.-C. Kim, B.-H. Choi, B.-K. Jeong, S.-H. Park, and K.-H. Lee, J. Electrochem. Soc. **151**, C52 (2004).
[30]J.-C. Kwak, Y.-H. Lee, and B.-H. Choi, Appl. Surf. Sci. **230**, 249 (2004).
[31]S. K. Kim, S. Hoffmann-Eifert, and R. Waser, Electrochem. Solid-State Lett. **14**, H146 (2011).
[32]S. Y. No, D. Eom, C. S. Hwang, and H. J. Kim, J. Electrochem. Soc. **153**, F87 (2006).
[33]M. B. M. Mousa, C. J. Oldham, and G. N. Parsons, Langmuir **30**, 3741 (2014).
[34]J. F. Conley, Jr., P. M. Lenahan, A. J. Lelis, and T. R. Oldham, Appl. Phys. Lett. **67**, 2179 (1995).
[35]H. H. Sønsteby, A. Yanguas-Gil, and J. W. Elam, J. Vac. Sci. Technol. A **38**, 020804 (2020).
[36]A. W. Ott, J. W. Klaus, J. M. Johnson, and S. M. George, Thin Solid Films **292**, 135 (1997).
[37]D. Z. Austin, K. E. K. Holden, J. Hinz, and J. F. Conley, Jr., Appl. Phys. Lett. **110**, 263503 (2017).
[38]N. Alimardani, S. W. King, B. L. French, C. Tan, B. P. Lampert, and J. F. Conley, Jr., J. Appl. Phys. **116**, 024508 (2014).
[39]M. D. Groner, J. W. Elam, F. H. Fabreguette, and S. M. George, Thin Solid Films **413**, 186 (2002).
[40]P. Gonon and C. Vallée, Appl. Phys. Lett. **90**, 142906 (2007).
[41]C. Besset, S. Bruyère, S. Blonkowski, S. Crémer, and E. Vincent, Microelectron. Rel. **43**, 1237 (2003).
[42]K. E. K. Holden, Y. Qi, and J. F. Conley, Jr., J. Appl. Phys. **129**, 144502 (2021).
[43]T. R. Oldham, *Ionizing Radiation Effects in MOS Oxides* (World Scientific, Singapore, 2000).
[44]J. F. Conley, Jr., P. M. Lenahan, A. J. Lelis, and T. R. Oldham, IEEE Trans. Nucl. Sci. **42**, 1744 (1995).
[45]Y. Zhang and M. Stuke, Jpn. J. Appl. Phys. **27**, L1349 (1988).
[46]K. E. K. Holden, G. D. R. Hall, M. Cook, C. Kendrick, K. Pabst, B. Greenwood, R. Daugherty, J. P. Gambino, and D. D. J. Allman, *2021 IEEE International Reliability Physics Symposium (IRPS)* (IEEE, 2021), pp. 1–10.
[47]F. Argall and A. K. Jonscher, Thin Solid Films **2**, 185 (1968).
[48]See supplementary material at https://www.scitation.org/doi/suppl/10.1116/6.0001865 for thermocouple wafer measurement tests with and without lamp exposure.